A MODEL BASED TECHNIQUE FOR FLIGHT DIRECTOR DESIGN: HELICOPTER HOVERING FLIGHT

Anthony John Palazzo

Library
Naval Postgraduate School
Monterey, California 93940

NAVAL POSTGRADUATE SCHOOL
Monterey, California

THESIS

A MODEL BASED TECHNIQUE
FOR FLIGHT DIRECTOR DESIGN:
HELICOPTER HOVERING FLIGHT

by

Anthony John Palazzo, Jr.

March 1975

Thesis Advisor: R.A. Hess

Approved for public release; distribution unlimited.

T167975

REPORT DOCUMENTATION PAGE

READ INSTRUCTIONS BEFORE COMPLETING FORM

1. REPORT NUMBER	2. GOVT ACCESSION NO. / 3. RECIPIENT'S CATALOG NUMBER
4. TITLE (and Subtitle): A Model Based Technique for Flight Director Design: Helicopter Hovering Flight	5. TYPE OF REPORT & PERIOD COVERED: Master's Thesis; March 1975
	6. PERFORMING ORG. REPORT NUMBER
7. AUTHOR(s): Anthony John Palazzo, Jr.	8. CONTRACT OR GRANT NUMBER(s)
9. PERFORMING ORGANIZATION NAME AND ADDRESS: Naval Postgraduate School, Monterey, California 93940	10. PROGRAM ELEMENT, PROJECT, TASK AREA & WORK UNIT NUMBERS
11. CONTROLLING OFFICE NAME AND ADDRESS: Naval Postgraduate School, Monterey, California 93940	12. REPORT DATE: March 1975
	13. NUMBER OF PAGES: 50
14. MONITORING AGENCY NAME & ADDRESS (if different from Controlling Office)	15. SECURITY CLASS. (of this report): Unclassified
	15a. DECLASSIFICATION/DOWNGRADING SCHEDULE

16. DISTRIBUTION STATEMENT (of this Report)

Approved for public release; distribution unlimited.

17. DISTRIBUTION STATEMENT (of the abstract entered in Block 20, if different from Report)

18. SUPPLEMENTARY NOTES

19. KEY WORDS (Continue on reverse side if necessary and identify by block number)

Optimal Control
Pilot Modeling
Flight Director Laws

20. ABSTRACT (Continue on reverse side if necessary and identify by block number)

A computer-aided Optimal Pilot Modeling Procedure was utilized to develop flight director laws for implementation in the longitudinal mode of a "head-down" cockpit display for a vertical take-off and landing aircraft. These flight director laws were intended to enhance the instrument hover and landing capabilities of the Bell UH-1H helicopter equipped with a multi-function stroke-written cathode ray

(20. ABSTRACT CONTINUED)

tube display.

A Model Based Technique for Flight Director Design: Helicopter Hovering Flight

by

Anthony John Palazzo, Jr.
Lieutenant, United States Navy
B.S., United States Naval Academy, 1966

Submitted in partial fulfillment of the
requirements for the degree of

MASTER OF SCIENCE IN AERONAUTICAL ENGINEERING

from the

NAVAL POSTGRADUATE SCHOOL
March 1975

Thesis
P1467
c.1

Library
Naval Postgradu
Monterey, Califor

ABSTRACT

A computer-aided Optimal Pilot Modeling Procedure was utilized to develop flight director laws for implementation in the longitudinal mode of a "head-down" cockpit display for a vertical take-off and landing aircraft. These flight director laws were intended to enhance the instrument hover and landing capabilities of the Bell UH-1H helicopter equipped with a multi-function stroke-written cathode ray tube display.

TABLE OF CONTENTS

I. INTRODUCTION ---------- 9

II. DEVELOPMENT OF THE HESS V/STOLAND DISPLAY ------- 11

III. DEVELOPMENT OF THE THEORETICAL MODEL ---------- 13

A. PILOT MODELING ---------- 13

B. VEHICLE MODEL ---------- 14

C. TURBULENCE MODEL ---------- 15

D. PILOT-VEHICLE SYSTEM MODEL ---------- 16

IV. THE OPTIMAL CONTROL-ESTIMATION PROBLEM ---------- 17

V. THE PILOT VEHICLE MODEL ---------- 23

VI. FLIGHT DIRECTOR LAWS ---------- 26

VII. CONCLUSIONS ---------- 28

VIII. RECOMMENDATIONS ---------- 29

APPENDIX A: TABLES ---------- 30

APPENDIX B: FIGURES ---------- 43

LIST OF REFERENCES ---------- 49

INITIAL DISTRIBUTION LIST ---------- 50

LIST OF FIGURES

1. Hess V/STOLAND Display Symbology ---------- 43

2. Block Diagram for the Pilot-Vehicle System Model --- 45

3. $\frac{\delta_B}{u}(s)$ Pilot Transfer Function ---------- 46

4. Relationship Between Vehicle Motion Variables and Cyclic Control Motions ---------- 47

5. Relationship Between Vehicle Motion Variables and Pilot Collective Control Motions ---------- 48

LIST OF TABLES

1. Pilot Model Parameters ---------- 30
2. Longitudinal Helicopter Equations of Motion -------- 31
3. Atmospheric Turbulence Model ---------- 32
4. System Equations for the Optimal Control and Estimation Problem ---------- 33
5. $\underline{A}$ Matrix ---------- 34
6. $\underline{x}$, $\underline{B}$, and $\underline{\gamma}$ Matrices ---------- 35
7. $\underline{y}$ and $\underline{C}$ Matrices ---------- 36
8. Displayed Variables ---------- 37
9. $\underline{H}$ Matrix ---------- 38
10. $\underline{w}$, $\underline{F}$, $\underline{v}$, $\underline{G}$, and $\underline{^{z}p}$ Matrices ---------- 39
11. $\underline{Q}$ and $\underline{R}$ Matrices ---------- 40
12. Parameter Values ---------- 41
13. Flight Director Gains ---------- 42

ACKNOWLEDGMENTS

The author wishes to express his sincere appreciation to the following organizations and people for their assistance during the course of this report:

Guidance and Navigation Branch, Ames Research Center, National Aeronautics and Space Administration, and in particular Mr. George Xenakis, for their support and valuable technical assistance.

Assistant Professor R. A. Hess, for his guidance and instruction as thesis advisor, and in particular for his support and encouragement as a friend.

My wife Helen and my three sons who had the patience to tolerate me throughout this endeavor.

I. INTRODUCTION

Increasing emphasis is being placed on the development of vertical and short-field take-off and landing type aircraft. Of those that have been developed few, if any, have a satisfactory instrument capability. The conventional presentation of flight information is simply insufficient for the transition to hover flight, particularly in limited access landing situations.

Current efforts to alleviate this deficiency have been most successful in the area of electronic displays. One such display is the Hess V/STOLAND display developed at the Ames Research Center of the National Aeronautics and Space Administration by Professor R. A. Hess. This display presents collocated conventional flight information for the initial phase of the approach and integrated contact situation information for the transition and hover phase. Implementation and evaluation by this author has resulted in various minor adjustments and modifications. For optimum effectiveness, however, a flight director system should be incorporated. A flight director system consists of display symbols which indicate desired movement of the pilot's controls, and the so-called flight director laws which drive these symbols as a function of aircraft deviations from a prescribed operating point.

It is the purpose of this thesis to design the flight director laws for the longitudinal mode of the UH-1H helicopter in hover using the Hess V/STOLAND display.

II. DEVELOPMENT OF THE HESS V/STOLAND DISPLAY

It is the opinion of the author that a "head-down" VTOL landing display must provide a realistic representation of the actual visual world. This opinion was confirmed with the modification and evaluation of the Hess V/STOLAND display during an effort to enhance its capabilities in the hover and landing mode.

The display was flown by the author in a fixed-based, digital simulation of the Bell UH-1H helicopter at the Ames Research Center. THe UH-1H is a single lifting rotor helicopter with stabilizer bar and conventional tail rotor, but without a stability augmentation system. Hover and landing transitions from a straight-in approach were made in order to ascertain both the accuracy and the confidence of the pilot with the display.

Presentations were made on a Sperry Flight System stroke-written multifunction display (MFD) with visual references provided by TV simulation of an actual airport environment.

Enclosure (5) of reference [2], an excerpt from "V/STOLAND MFD Display for Research Computer" by R. L. Sharp, represented the original display of Professor R. A. Hess. The hover mode of this display is shown in Figure 1. The ensuing development in [2] incorporated revisions by Professor Hess, and further changes made by the author during implementation. (Note that the flight director symbols

indicated were not operative.) This display provided satisfactory results during the approach phase, but proved somewhat inadequate during the transition and hover phase. A well designed flight director could alleviate this inadequacy.

In the final analysis the Hess V/STOLAND display seemed highly adaptable for shipboard use due to its ability to present a dual perspective view of the landing situation, and through its potential to maintain the necessary flight control sensitivity for limited access landings through the use of a flight director system.

III. DEVELOPMENT OF THE THEORETICAL MODEL

A. PILOT MODELING

The modeling hypothesis utilized for this development is that, subject to his inherent limitations, the well-trained well-motivated pilot behaves in an optimal manner. The pilot's control characteristics can be modeled by the solution of an optimal linear control problem and optimal estimation problem with certain "modifications". These pilot modifications are:

1. time delay - a pure time delay is included in each of the pilot's control outputs.

2. neuromuscular dynamics - each output neuromuscular system is modeled as a first order lag.

3. observation noise and motor noise - each observed variable is assumed to contain pilot induced additive white noise which scales with the variance of the observed variable; each control output is assumed to contain pilot induced additive white noise which scales with the variance of the control motion.

4. if a variable is displayed explicitly, the pilot also perceives the first derivative of the variable but no higher derivatives. The first derivative is also noise contaminated.

5. the index of performance for the optimization procedure is chosen subjectively to mirror what the display system designer believes to be the task and control objectives as perceived by the pilot.

The time delay of the pilot is modeled through the use of a second order Pade' approximation, which permits direct implementation of the computer-aided optimal pilot modeling procedure. Table 1 presents the complete list of pilot modeling parameters. These parameter values, as well as the form of the observation and motor noise covariances have been well documented in the literature e.g. Refs. 1 and 3.

B. VEHICLE MODEL

The vehicle model used was the unaugmented UH-1H helicopter with a single lifting rotor with stabilization bar, a device attached to the rotor hub which provides pitch and roll damping, and a conventional tail rotor. The following assumptions were made:

1. the vehicle was an idealized rigid airframe with a rotor attached.

2. the rotor was described by the tip path plane whose orientation determines the propulsive and aerodynamic forces and moments.

3. no rotor degrees of freedom are considered other than the control inputs which serve to describe the instantaneous tip path plane orientation.

4. all coupling between the longitudinal and lateral motion is ignored.

5. linearized small perturbation motion about the horizontal reference flight path is assumed.

The longitudinal equations of motion for the UH-1H are presented in Table 2.

C. TURBULENCE MODEL

In aircraft stability and control analysis, gusts often play an important role. Accordingly, the most sophisticated and realistic treatment of gust disturbances should be employed. Therefore, the stochastic approach was adopted in which the gust velocity in any direction at any fixed point in space is considered to be random in nature. Reference [4] suggest the use of the simplified spectrum for flight control system analysis presented in Table 3. There is no theoretical basis for this form, but its agreement with measured spectra, the preservation of the characteristic length, L_u, and its simplicity suggest its use. For these reasons this spectrum was chosen for the development presented here. It should be noted that for development of the hover mode flight director, only the horizontal turbulence will be considered. Strong rotor downwash, produced by high power requirements for hover flight in close ground proximity, tend to negate any effects of vertical turbulence. Also, since the simplified spectrum form has been normalized to the reference airspeed (U_o), hover flight would theoretically have no turbulence. This, in fact, is not the case; therefore a reference airspeed of 20 knots (<u>for turbulence modeling only</u>) has been introduced.

D. PILOT-VEHICLE SYSTEM MODEL

The Pilot-Vehicle System Model depicted in Figure 2 represents the optimal control and estimation model used for the development of this study, and Table 4 contains the system equations. As Figure 2 indicates, the vehicle is disturbed from the steady hover operating point by the horizontal turbulence. Linear functions of the system states are displayed to the pilot in the cockpit. The pilot then operates upon these displayed variables and generates corrective control outputs. It is assumed that the manner in which the pilot operates on the displayed variables can be modeled by an optimal estimator and a state feedback controller. The optimal state feedback control, u(t), is then delayed, summed with the pilot white motor noise, and passed through the neuromuscular dynamics to form the pilot control motions.

IV. THE OPTIMAL CONTROL-ESTIMATION PROBLEM

Before discussing the specifics of the pilot modeling procedure, a review of the optimal control-estimation problem is in order. This problem can be outlined as follows:

Consider a system described by

$$\dot{\underline{x}}(t) = \underline{A}\,\underline{x}(t) + \underline{B}\,\underline{u}(t) + \underline{\gamma}\,\underline{w}(t)$$

$$\underline{y}(t) = \underline{C}\,\underline{x}(t)$$

where

$\underline{A}$	is an n x n plant matrix
$\underline{x}(t)$	is an n x 1 state vector
$\underline{B}$	is an n x p control matrix
$\underline{u}(t)$	is a p x 1 control vector
$\underline{\gamma}$	is an n x t disturbance matrix
$\underline{w}(t)$	is a t x 1 disturbance vector
$\underline{y}(t)$	is a q x 1 output vector
$\underline{C}$	is a q x n output matrix

Here, $\underline{w}(t)$ is a vector of linearly uncorrelated, zero mean white noise signals with Gaussian amplitude probability distribution functions. The elements of $\underline{w}(t)$ are assumed to

be sample functions from n random processes which are each ergodic and are jointly ergodic. The covariance matrix for $\underline{w}(t)$ is

$$E[\underline{w}(t)\ \underline{w}^T(t+\tau)] = \underline{F}\ \delta(\tau)$$

where $\delta(\tau)$ is the unit impulse function.

The measured quantities or sensor signals are

$$\underline{z}(t) = \underline{H}\ \underline{w}(t) + \underline{v}(t)$$

where

$\underline{z}(t)$ is a u x 1 measurement vector

$\underline{H}$ is a u x n measurement matrix

$\underline{v}(t)$ is a u x 1 measurement noise vector

The elements of $\underline{v}(t)$ are assumed to be sample functions from p random processes each of which are ergodic and jointly ergodic. The covariance matrix for $\underline{v}(t)$ is

$$E[\underline{v}(t)\ \underline{v}^T(t+\tau)] = \underline{G}\ \delta(t)$$

The system is assumed to be completely controllable and completely observable. It is desired to find the control function $\underline{u}(t)$ which minimizes the quadratic scalar index of performance

$$J \lim_{T\to\infty} 1/T \int_0^T [\underline{y}^T(t)\ \underline{Q}\ \underline{y}(t) + \underline{u}^T(t)\ \underline{R}\ \underline{u}(t)]\ dt$$

where

$\underline{Q}$ is a q x q symmetric output cost weighting matrix and at least positive semidefinite

$\underline{R}$ is a p x p symmetric control cost weighting matrix and positive definite

The solution to the linear quadratic Gaussian control problem can be outlined as follows:

1. The optimization problem can, by the called Separation Theorem, be broken up into two separate problems, an optimal control problem and an optimal estimation or filtering problem.

2. The optimal estimation or filtering problem generates an optimal estimate, $\hat{\underline{x}}(t)$, of the state $\underline{x}(t)$. This estimate is optimal in the sense that

$$\lim_{T\to\infty} 1/T \int_0^T \tilde{\underline{x}}^T(t)\ \tilde{\underline{x}}(t)\ dt$$

is minimized, where $\tilde{x}(t)$ is the estimation error defined as

$$\tilde{\underline{x}}(t) = \hat{\underline{x}}(t) - \underline{x}(t)$$

The optimal estimator (or Kalman filter) has the form

$$\dot{\hat{\underline{x}}}(t) = \underline{A}\ \hat{\underline{x}}(t) + \underline{B}\ \underline{u}(t) + \underline{K}[\underline{z}(t) - \underline{H}\ \hat{\underline{x}}(t)]$$

The estimator gains are given by

$$\underline{K} = \underline{P}\ \underline{H}^T\ \underline{G}^{-1}$$

where $\underline{P}$ is the error covariance matrix

$$E[\tilde{\underline{x}}(t)\ \tilde{\underline{x}}^T(t + \tau)] = \underline{P}\ \delta(t)$$

$\underline{P}$ is the positive definite solution to the steady-state filter matrix Riccati equation

$$\underline{A}\ \underline{P} + \underline{P}\ \underline{A}^T + \underline{\gamma}\ \underline{F}\ \underline{\gamma}^T - \underline{P}\ \underline{H}^T\ \underline{G}^{-1}\ \underline{H}\ \underline{P} = 0$$

3. The optimal control problem generates an optimal control law $\underline{u}(t)$ which is a linear function of the estimated state

$$\underline{u}(t) = -\ \underline{L}\ \hat{\underline{x}}(t)$$

where $\underline{L}$ is a p x n optimal controller gain matrix. The gain matrix $\underline{L}$ is identical to the one obtained by solving the optimal control problem with no system disturbance, exact state information, and the index of performance given by

$$J \int_0^\infty [\underline{y}^T(t)\ \underline{Q}\ \underline{y}(t) + \underline{u}^T(t)\ \underline{R}\ \underline{u}(t)]\ dt$$

The controller gain matrix $\underline{L}$ is given by

$$\underline{L} = \underline{R}^{-1} \underline{B}^T \underline{S}$$

where $\underline{S}$ is the positive definite solution to the steady-state control matrix Riccati equation

$$- \underline{S} \underline{A} - \underline{A}^T \underline{S} - \underline{C}^T \underline{Q} \underline{C} + \underline{S} \underline{B} \underline{R}^{-1} \underline{B}^T \underline{S} = 0$$

It can be shown that the state covariance matrix

$$E[\underline{x}(t) \underline{x}^T(t + \tau)] = (\underline{P} + \underline{M}) \delta(\tau)$$

where $\underline{P}$ is the solution to the filter matrix Riccati equation and $\underline{M}$ is the positive definite solution to

$$(\underline{A} - \underline{B} \underline{L}) \underline{M} + \underline{M} (\underline{A} - \underline{B} \underline{L})^T + \underline{K} \underline{G} \underline{K}^T = 0$$

In addition to the solutions outlined above, it can be shown that the transfer matrix relating the Laplace transform of the optimal control law $\underline{u}(t)$ to the Laplace transform of the measurement vector $\underline{z}(t)$ (with $\underline{v}(t) \equiv 0$) is given by

$$\underline{U}(S) = - \underline{L} (S\underline{I} - \underline{A} + \underline{B} \underline{L} + \underline{K} \underline{H})^{-1} \underline{K} \underline{Z}(S)$$

where

$$\underline{U}(S) = \mathcal{L}[\underline{u}(t)]$$

$$\underline{Z}(S) = \mathcal{L}[\underline{z}(t)]$$

V. PILOT-VEHICLE MODEL

The equations of Table 4 are specialized as follows: the 13 differential equations describing the "plant" consist of the six vehicle state equations involving the state variables

- u - groundspeed
- w - velocity in the z stability axis direction
- q - pitch rate
- θ - pitch angle
- h - altitude deviation
- x - longitudinal displacement from the pad

In addition, a state u_g is added which represents the longitudinal turbulence. This u_g represents the output of a shaping filter excited by white noise and has the power spectral density given in Table 3.

Four additional states $d_1 \rightarrow d_4$, were necessary for the second order Pade' approximation for the pilot's effective time delay for each control.

Finally, two states δ_B and δ_C, representing the pilot's cyclic and collective control motions, respectively, were formed. These states resulted when the first order neuromuscular dynamics were put in state format. The $\underline{A}$, $\underline{B}$, and $\underline{\gamma}$ matrices are shown in Tables 5 and 6.

The output variables, $\underline{y}(t)$ are

$$y_1 = u$$
$$y_2 = q$$
$$y_3 = h$$
$$y_4 = x$$

Table 7 gives the corresponding $\underline{C}$ matrix. The displayed variables, $\underline{z}_p(t)$ are given in Table 8, while Table 9 gives the $\underline{H}$ matrix.

The covariance of $\underline{F}$ and $\underline{G}$ are given in Table 10. Note that all but one of the elements of $\underline{F}$ and $\underline{G}$ depend upon the variances of system variables. These variances, however, are not known *a priori*. Hence an iterative solution is necessary. Initial guesses are made for the variances, a solution is obtained, the resulting variances used, and a new solution obtained, etc. As pointed out in Ref. [1], the number of iterations necessary for a final solution is roughly twice the number of displayed or perceived variables, in this case 2 x 6 = 12.

The $\underline{Q}$ and $\underline{R}$ matrices are shown in Table 11. The elements of these matrices are the squares of the reciprocals of the "maximum allowable" deviations of the output quantities. Thus, when any output variable attains the allowable limits, it makes a contribution of unity to the integrand of the index of performance. Table 12 lists these maximum allowable limits chosen subjectively for the particular vehicle and task under study.

The optimal control and estimation problem was solved using a modified form of VASP (Ref. [5]) on the Naval Postgraduate School IBM 360 computer.

VI. FLIGHT DIRECTOR LAWS

From the output of the final iteration of the modeling procedure, 12 pilot "transfer functions" were obtained. These 12 functions relate the Laplace transform of the cyclic and collective control motions to the transforms of the six displayed or perceived variables.

The amplitude ratio plot of one such transfer function

$$\frac{\delta_B}{u}(s)$$

is shown in Figure 3. Each of the 12 transfer functions exhibited similar frequency characteristics. The similarity included break frequencies and high frequency asymptotes. Pure gain approximations were made to the Bode diagrams as shown in Figure 3. These gains were normalized with respect to the largest magnitude in each set of six to obtain the flight director gains of Table 13. These gains can be used to generate the director laws according to

$$\delta_B' = K_{B_x} x + K_{B_u} u + K_{B_\theta} \theta + K_{B_q} q + K_{B_h} h + K_{B_{\dot{h}}} \dot{h}$$

$$\delta_C' = K_{C_x} x + K_{C_u} u + K_{C_\theta} \theta + K_{C_q} q + K_{C_h} h + K_{C_{\dot{h}}} \dot{h}$$

The normalized Bode gains of the pilot transfer functions (Table 13) and the RMS values of the six vehicle motion

variables were then used to qualitatively assess the extent to which each motion variable affects each of the two pilot control outputs. Figures 4 and 5 were obtained by multiplying the RMS values of each of the six vehicle motion variables displayed or perceived by the pilot by the Bode gains of the respective transfer function for the cyclic or collective control, and normalizing to the largest value obtained for each control. The bars in Figures 4 and 5 can be thought of as representing approximations to the relative amount of power in the cyclic or collective output which can be associated with the vehicle motion variable indicated.

Figures 4 and 5 indicate that height deviation, pitch rate, height deviation rate, and pitch deviations, in order of importance are associated with cyclic control; while pitch rate, height deviation rate, pitch, height deviation, and groundspeed deviations, in order of importance, are associated with collective control.

VII. CONCLUSIONS

Intuitively, one would assume that cyclic motion in a hover would primarily be determined by groundspeed, range, pitch, and pitch rate in that order, with little effect shown by height deviation or height deviation rate. Figure 4 shows however, that for this study, height deviation is of primary importance, with pitch rate, height deviation rate, and pitch making minor contributions. Similarly, one would expect collective motion to be determined by height deviation and height deviation rate primarily, but Figure 5 presents pitch rate as being the primary stimulus, with height deviation rate, pitch, and height deviation making major contributions, and groundspeed having a minor effect.

Although the analytical results seem in opposition to those obtained by intuitive reasoning, only pilot-in-the-loop simulation will provide definitive answers regarding the efficiency of the director laws.

VIII. RECOMMENDATIONS

The flight director laws resulting from this study should be displayed under simulation and evaluated as to their effectiveness. For comparison, additional studies should be made using varied modeling parameters and weighting functions. One such set of weighting functions could be obtained by setting the maximum allowable values in $\underline{Q}$ and $\underline{R}$ equal to the respective RMS values obtained in the modeling procedure.

APPENDIX A. TABLES

TABLE 1. Pilot Model Parameters

Time delay	$e^{-\tau s}$	$\tau = 0.3$ secs.
Neuromuscular system	$\frac{1}{T_N s + 1}$	$T_N = 0.2$ secs.
Observation noise	V_{z_i}	$V_{z_i} = \rho \pi E[z_{p_i}^2(t)]$ $\rho = 0.1$
Motor noise	α_i	$\alpha_i^2 = \rho' \pi E[u_{i-1}^2(t)]$ $(i=2,3)$ $\rho' = 0.01$
Index of performance	J	$J = \lim_{T \to \infty} \frac{1}{T} \int_0^T [\underline{y}^T(t)\ \underline{Q}\ \underline{y}(t) + \underline{u}^T(t)\ \underline{R}\ \underline{u}(t)]dt$

TABLE 2.

Longitudinal Helicopter Equations of Motion

$$\dot{u} = X_u u + X_w w + X_q q - g\theta + 0 + X_{\delta_B}\delta_B + X_{\delta_C}\delta_C - X_u u_g$$

$$\dot{w} = Z_u u + Z_w w + (U_o + Z_q) q + 0 + 0 + Z_{\delta_B}\delta_B + Z_{\delta_C}\delta_C - Z_u u_g$$

$$\dot{q} = (M_u + M_{\dot{w}} Z_u) u + (M_w + M_{\dot{w}} Z_w) w + [M_q + M_{\dot{w}} (U_o + Z_q)] q + 0 + 0 + (M_{\delta_B} + M_{\dot{w}} Z_{\delta_B})\delta_B + (M_{\delta_C} + M_{\dot{w}} Z_{\delta_C})\delta_C - (M_u + M_{\dot{w}} Z_u) u_g$$

$$\dot{\theta} = 0 + 0 + 1.0q + 0 + 0 + 0 + 0 + 0$$

$$\dot{h} = 0 - 1.0w + 0 + U_o\theta + 0 + 0 + 0 + 0$$

$$\dot{x} = u + 0 + 0 + 0 + 0 + 0 + 0 + 0$$

TABLE 3

Atmospheric Turbulence Model

$$\Phi_{u_g u_g}(\omega) = \frac{2\sigma_u^2 U_o}{L_u} \frac{1}{\omega^2 + \frac{U_o^2}{L_u^2}}$$

$$\alpha_1 = \sqrt{\frac{2U_o}{L_u}}\ \sigma_u$$

$$\beta_1 = \frac{U_o}{L_u}$$

L_u = 600 ft.

U_o = 20 knots (for turbulence modeling only)

σ_u = 5 ft/sec.

TABLE 4

System Equations for the Optimal Control and Estimation Problem

$$\dot{\underline{x}}(t) = \underline{A}\ \underline{x}(t) + \underline{B}\ \underline{u}(t) + \underline{\gamma}\ \underline{w}(t)$$

$$\underline{y}(t) = \underline{C}\ \underline{x}(t)$$

$$\underline{z}(t) = \underline{H}\ \underline{x}(t) + \underline{v}(t) = \underline{z_p}(t) + \underline{v}(t)$$

$$E[\underline{w}(t)\ \underline{w}^T(t+\tau)] = \underline{F}\ \delta(\tau)$$

$$E[\underline{v}(t)\ \underline{v}^T(t+\tau)] = \underline{G}\ \delta(\tau)$$

$$J = \lim_{T\to\infty} \frac{1}{T} \int_0^T [\underline{y}^T(t)\ \underline{Q}\ \underline{y}(t) + \underline{u}^T(t)\ \underline{R}\ \underline{u}(t)]\ dt$$

TABLE 5 $\underline{A}$ Matrix

X_u	X_w	X_q	$-g$	0	0	$-X_u$	0	0	X_{δ_B}	0	0	X_{δ_C}
Z_u	Z_w	U_o+Z_q	0	0	0	$-Z_u$	0	0	Z_{δ_B}	0	0	Z_{δ_C}
$M_u+M_{\dot{w}}Z_u$	$M_w+M_{\dot{w}}Z_w$	$M_q + M_{\dot{w}}(U_o+Z_q)$	0	0	0	$-(M_u+M_{\dot{w}}Z_u)$	0	0	$M_{\delta_B}+M_{\dot{w}}Z_{\delta_B}$	0	0	$M_{\delta_C}+M_{\dot{w}}Z_{\delta_C}$
0	0	1.0	0	0	0	0	0	0	0	0	0	0
0	-1.0	0	U_o	0	0	0	0	0	0	0	0	0
1.0	0	0	0	0	0	0	0	0	0	0	0	0
0	0	0	0	0	0	$-\beta_1$	0	0	0	0	0	0
0	0	0	0	0	0	0	0	1.0	0	0	0	0
0	0	0	0	0	0	0	$-(\frac{16}{\tau^2})$	$-(\frac{8}{\tau})$	0	0	0	0
0	0	0	0	0	0	0	$\frac{1}{T_N}$	0	$-(\frac{1}{T_N})$	0	0	0
0	0	0	0	0	0	0	0	0	0	0	1.0	0
0	0	0	0	0	0	0	0	0	0	$-(\frac{16}{\tau^2})$	$-(\frac{8}{\tau})$	0
0	0	0	0	0	0	0	0	0	0	$\frac{1}{T_N}$	0	$-(\frac{1}{T_N})$

TABLE 6

$\underline{x}$ Matrix

$$\begin{bmatrix} u \\ w \\ q \\ \theta \\ h \\ x \\ u_g \\ d_1 \\ d_2 \\ \delta_B \\ d_3 \\ d_4 \\ \delta_C \end{bmatrix}$$

$\underline{B}$ Matrix

$$\begin{bmatrix} 0 & 0 \\ 0 & 0 \\ 0 & 0 \\ 0 & 0 \\ 0 & 0 \\ 0 & 0 \\ 0 & 0 \\ -\left(\frac{16}{\tau}\right) & 0 \\ \frac{128}{\tau^2} & 0 \\ \frac{\tau}{T_N} & 0 \\ 0 & -\left(\frac{16}{\tau}\right) \\ 0 & \frac{128}{\tau^2} \\ 0 & \frac{1}{T_N} \end{bmatrix}$$

$\underline{\gamma}$ Matrix

$$\begin{bmatrix} 0 & 0 & 0 \\ 0 & 0 & 0 \\ 0 & 0 & 0 \\ 0 & 0 & 0 \\ 0 & 0 & 0 \\ 0 & 0 & 0 \\ 1.0 & 0 & 0 \\ 0 & 0 & 0 \\ 0 & 0 & 0 \\ 0 & \frac{1}{T_N} & 0 \\ 0 & 0 & 0 \\ 0 & 0 & 0 \\ 0 & 0 & \frac{1}{T_N} \end{bmatrix}$$

TABLE 7

$\underline{y}$ Matrix $\underline{C}$ Matrix

$$\begin{bmatrix} y_1 \\ y_2 \\ y_3 \\ y_4 \end{bmatrix} = \begin{bmatrix} 1 & 0 & 0 & 0 & 0 & 0 & 0 & 0 & 0 & 0 & 0 & 0 & 0 \\ 0 & 0 & 1 & 0 & 0 & 0 & 0 & 0 & 0 & 0 & 0 & 0 & 0 \\ 0 & 0 & 0 & 0 & 1 & 0 & 0 & 0 & 0 & 0 & 0 & 0 & 0 \\ 0 & 0 & 0 & 0 & 0 & 1 & 0 & 0 & 0 & 0 & 0 & 0 & 0 \end{bmatrix} \begin{bmatrix} \underline{x} \end{bmatrix}$$

TABLE 8

DISPLAYED VARIABLES

z_{p_1}	- displayed longitudinal displacement from touchdown point = $K_1 x$	(K_1 = .00133 rad/ft.)
z_{p_2}	- perceived time rate of change of longitudinal displacement from touchdown point = $K_2 u$	(K_2 = .003289 rad/ft/sec.)
z_{p_3}	- perceived time rate of change of height deviation = $K_3(-\omega + U_o\theta)$	(K_3 = .00133 rad/ft/sec.)
z_{p_4}	- perceived pitch rate = $K_4 q$	(K_4 = .0955 rad/rad/sec.)
z_{p_5}	- displayed pitch angle = $K_5\theta$	(K_5 = .0955 rad/rad)
z_{p_6}	- displayed height deviation = $K_6 h$	(K_6 = .00133 rad/ft.)

The K_i are display gains, e.g.

$$K_4 = |K_4| \frac{\text{radians subtended at the pilot's eye by the display element motion}}{\text{element's motion rate}}$$

TABLE 9

$\underline{H}$ Matrix

$$\begin{bmatrix} 0 & 0 & 0 & 0 & 0 & K_1 & 0 & 0 & 0 & 0 & 0 & 0 & 0 \\ K_2 & 0 & 0 & 0 & 0 & 0 & 0 & 0 & 0 & 0 & 0 & 0 & 0 \\ 0 & -K_3 & 0 & K_3U_o & 0 & 0 & 0 & 0 & 0 & 0 & 0 & 0 & 0 \\ 0 & 0 & K_4 & 0 & 0 & 0 & 0 & 0 & 0 & 0 & 0 & 0 & 0 \\ 0 & 0 & 0 & K_5 & 0 & 0 & 0 & 0 & 0 & 0 & 0 & 0 & 0 \\ 0 & 0 & 0 & 0 & K_6 & 0 & 0 & 0 & 0 & 0 & 0 & 0 & 0 \end{bmatrix}$$

TABLE 10

$\underline{w}$ Matrix

$$\begin{bmatrix} w_1 \\ w_2 \\ w_3 \end{bmatrix}$$

$\underline{F}$ matrix

$$\begin{bmatrix} \alpha_1^2 & 0 & 0 \\ 0 & \alpha_2^2 & 0 \\ 0 & 0 & \alpha_3^2 \end{bmatrix}$$

$$\alpha_2^2 = \rho' \pi E[u_1^2(t)]$$

$$\alpha_3^2 = \rho' \pi E[u_2^2(t)]$$

$\underline{v}$ Matrix

$$\begin{bmatrix} v_1 \\ v_2 \\ v_3 \\ v_4 \\ v_5 \\ v_6 \end{bmatrix}$$

$\underline{G}$ matrix

$$\begin{bmatrix} V_{z_1} & 0 & 0 & 0 & 0 & 0 \\ 0 & V_{z_2} & 0 & 0 & 0 & 0 \\ 0 & 0 & V_{z_3} & 0 & 0 & 0 \\ 0 & 0 & 0 & V_{z_4} & 0 & 0 \\ 0 & 0 & 0 & 0 & V_{z_5} & 0 \\ 0 & 0 & 0 & 0 & 0 & V_{z_6} \end{bmatrix}$$

$$V_{z_1} = \rho \pi E[z_{p_1}^2(t)]$$

$$V_{z_2} = \rho \pi E[z_{p_2}^2(t)]$$

$$V_{z_3} = \rho \pi E[z_{p_3}^2(t)]$$

$$V_{z_4} = \rho \pi E[z_{p_4}^2(t)]$$

$$V_{z_5} = \rho \pi E[z_{p_5}^2(t)]$$

$$V_{z_6} = \rho \pi E[z_{p_6}^2(t)]$$

$$\underline{z_p}(t) = \begin{bmatrix} z_{p_1}(t) \\ z_{p_2}(t) \\ z_{p_3}(t) \\ z_{p_4}(t) \\ z_{p_5}(t) \\ z_{p_6}(t) \end{bmatrix} = \underline{H}\, \underline{x}(t)$$

TABLE 11

$\underline{Q}$ Matrix

$$\begin{bmatrix} \left(\frac{1}{u_{max}}\right)^2 & 0 & 0 & 0 \\ 0 & \left(\frac{1}{g_{max}}\right)^2 & 0 & 0 \\ 0 & 0 & \left(\frac{1}{h_{max}}\right)^2 & 0 \\ 0 & 0 & 0 & \left(\frac{1}{x_{max}}\right)^2 \end{bmatrix}$$

$\underline{R}$ Matrix

$$\begin{bmatrix} \left(\frac{1}{\delta_{B_{max}}}\right)^2 & 0 \\ 0 & \left(\frac{1}{\delta_{C_{max}}}\right)^2 \end{bmatrix}$$

TABLE 12

Parameter Values (0 Knots)

U_o	=	0 ft/sec.
σ_u	=	5 ft/sec.
L_u	=	600 ft.
τ	=	0.3 sec.
T_N	=	0.2 sec.
K_1	=	.00133 rad/ft.
K_2	=	.003289 rad/ft/sec.
K_3	=	.00133 rad/ft/sec.
K_4	=	.0955 rad/rad/sec.
K_5	=	.0955 rad/rad.
K_6	=	.00133 rad/ft.
u_{max}	=	5.067 ft/sec. = 3 knots
q_{max}	=	.04 rad/sec.
h_{max}	=	10 ft.
N_{max}	=	25 ft.
$\delta_{B_{max}}$	=	.1 ft.
$\delta_{C_{max}}$	=	.1 ft.
ρ'	=	.01
ρ	=	.1

TABLE 13

Flight Director Gains

$K_{B_x} = -1.246 \times 10^{-4}$	$K_{C_x} = -1.99 \times 10^{-5}$
$K_{B_u} = -4.971 \times 10^{-5}$	$K_{C_u} = +1.343 \times 10^{-3}$
$K_{B_{\dot{h}}} = -4.151 \times 10^{-3}$	$K_{C_{\dot{h}}} = -3.675 \times 10^{-3}$
$K_{B_q} = -1$	$K_{C_q} = -1$
$K_{B_\theta} = -.3903$	$K_{C_\theta} = -.4645$
$K_{B_h} = -.0141$	$K_{C_h} = -1.177 \times 10^{-3}$

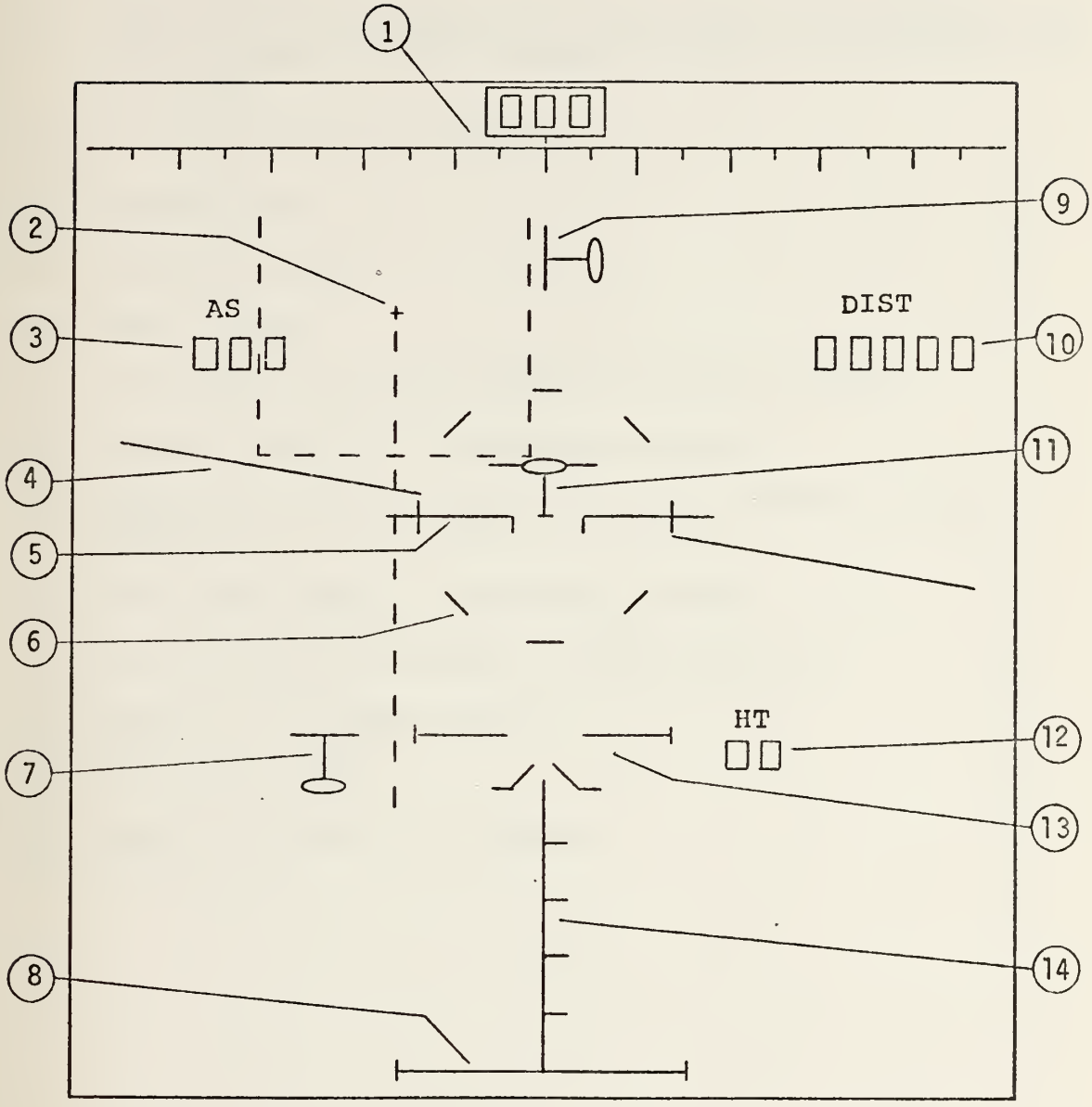

FIGURE 1. Hess V/STOLAND Display Symbology

FIGURE 1 KEY

1. Heading Tape
2. Center of the landing pad about which the landing pad is generated and the course line/lateral deviation line is fixed.
3. Air(Ground) Speed Digits
4. Horizon Bar
5. Aircraft Symbol
6. Rotor Symbol
7. Collective Steering Command (Flight Director)
8. Landing Pad (for glideslope deviation)
9. Heading Index and Rudder Steering Command (Flight Director)
10. Distance (range to touchdown) Digits
11. Cyclic Steering Command (Flight Director)
12. Height (altitude) Digits
13. Aircraft Symbol
14. Height Deviation Increments

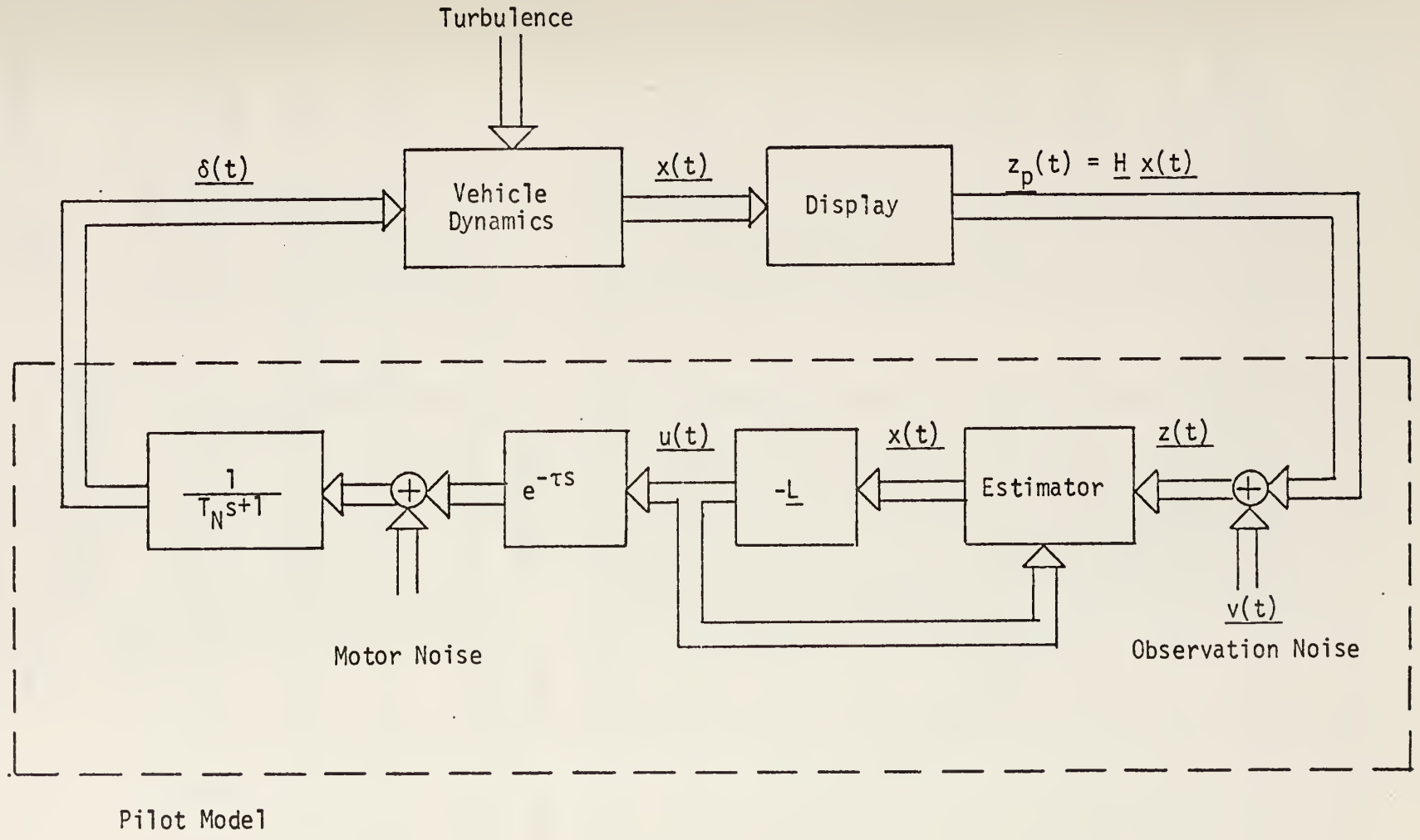

FIGURE 2. Block Diagram for the Pilot-Vehicle System Model

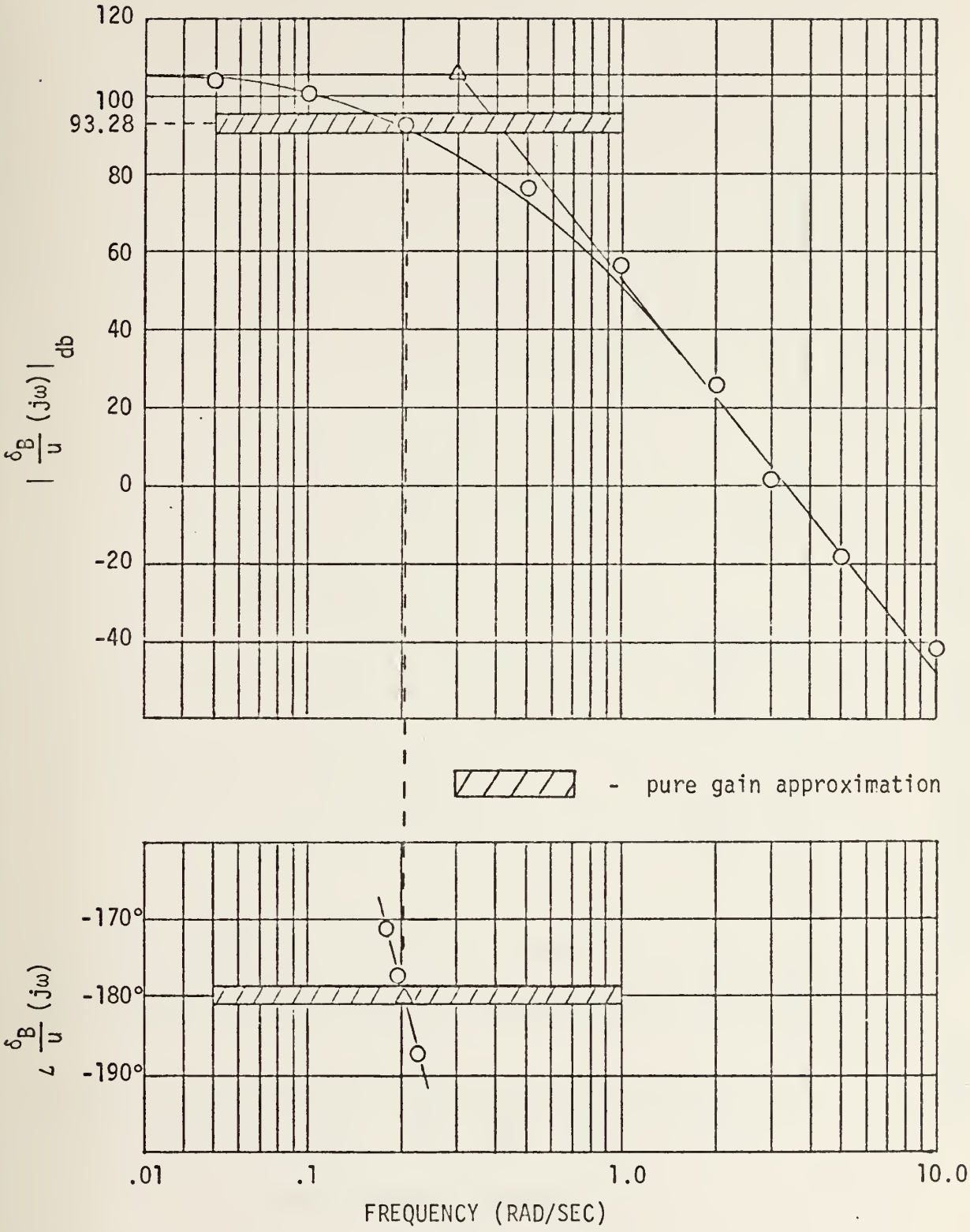

FIGURE 3. $\frac{\delta_B}{u}(s)$ Pilot Transfer Function

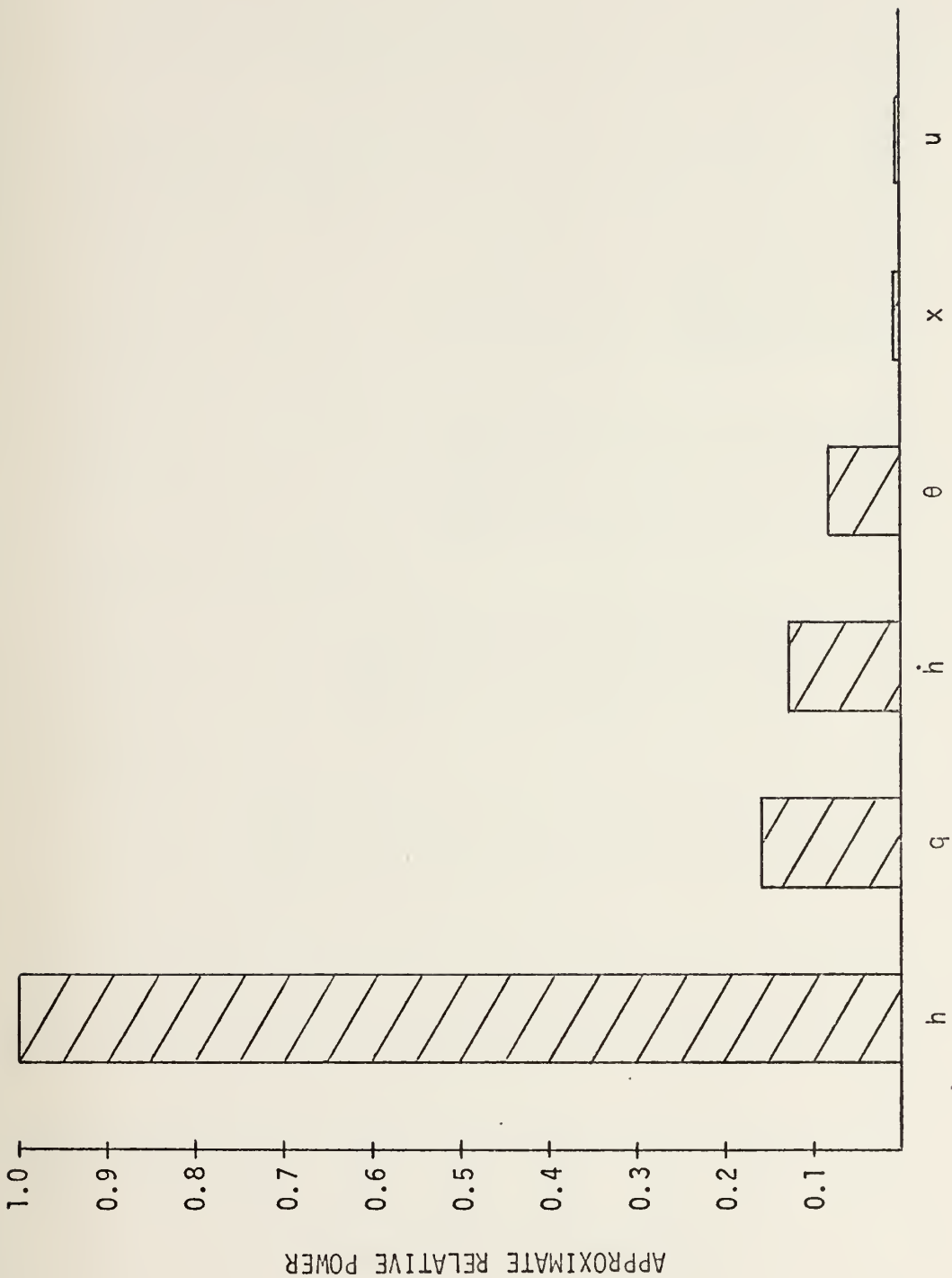

FIGURE 4. Relationship Between Vehicle Motion Variables and Cyclic Control Motions

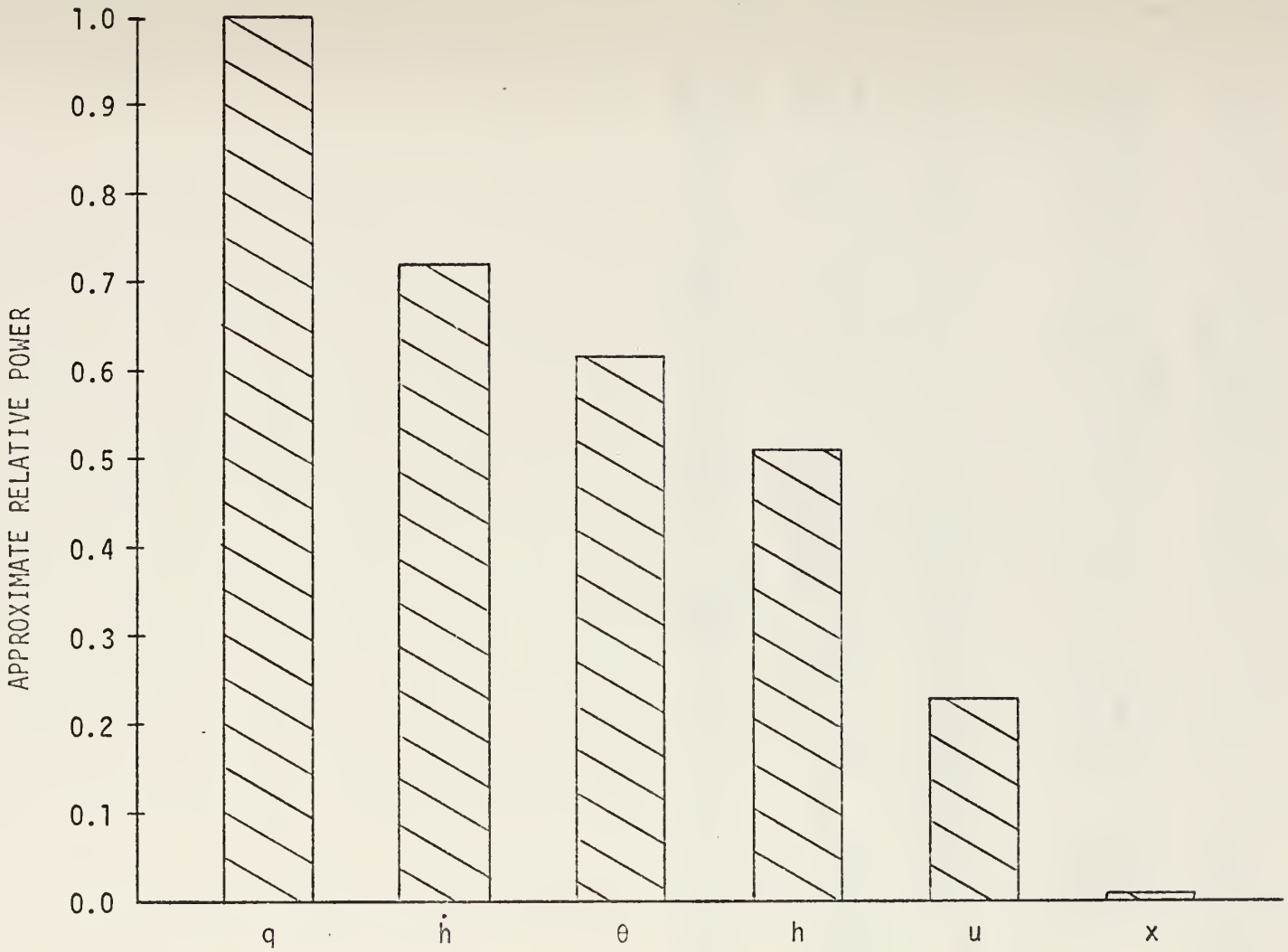

FIGURE 5. Relationship Between Vehicle Motion Variables and Pilot Collective Control Motions

LIST OF REFERENCES

1. Kleinman, D.L., Baron, S., and Levison, W.H., "An Optimal Model of Human Response, Part I: Theory and Validation," Automatica, v. 6, p. 357-369, May 1970.

2. Palazzo, A.J., "Report on the Evaluation of the Modified Poletrack Display and the Revised Hess V/STOLAND Display as of 14 February 1975," Naval Postgraduate School, Monterey, California, February 1975.

3. Levison, W.H., "A Model-Based Technique for the Design of Flight-Directors," Proceedings of 9th Annual Conference on Manual Control, p. 163-172, May 1973.

4. Hart, J.E., Adkins, L.A., and Lacau, L.L., "Stochastic Disturbance Data for Flight Control System Analysis," ASD - TDR - 62 - 347, September 1962.

5. White, J.S., and Lee, H.Q., "Users Manual for the Variable Dimension Automatic Synthesis Program (VASP)," NASA - TM - X 2417, October 1971.

INITIAL DISTRIBUTION LIST

		No. Copies
1.	Defense Documentation Center Cameron Station Alexandria, Virginia 22314	2
2.	Library, Code 0212 Naval Postgraduate School Monterey, California 93940	2
3.	Department Chairman, Code 57 Department of Aeronautics Naval Postgraduate School Monterey, California 93940	2
4.	Asst. Professor R.A. Hess, Code 57He Department of Aeronautics Naval Postgraduate School Monterey, California 93940	2
5.	LT Anthony John Palazzo, Jr. USN 1926A Sparrow Drive NAS Pt. Mugu, California 93042	3

160793
Thesis
P1428 Palazzo
c.1 A model based technique for flight director design: helicopter hovering flight.

160793
Thesis
P1428 Palazzo
c.1 A model based technique for flight director design: helicopter hovering flight.

thesP1428
A model based technique for flight direc
3 2768 001 97134 4
DUDLEY KNOX LIBRARY